ADVANCED HEALTHCARE MATERIALS

Supporting Information

for *Adv. Healthcare Mater.*, DOI 10.1002/adhm.202301610

High-Performance Artificial Ligament Made from Helical Polyester Fibers Wrapped with Aligned Carbon Nanotube Sheets

Liyuan Wang, Hongyu Jiang, Fang Wan, Hongji Sun, Yiqing Yang, Wenjun Li, Zheyan Qian, Xuemei Sun, Peining Chen*, Shiyi Chen and Huisheng Peng**

SUPPORTING INFORMATION

High-performance Artificial Ligament Made from Helical Polyester Fibers Wrapped with Aligned Carbon Nanotube Sheets

Liyuan Wang,[+[a]] Hongyu Jiang,[+[a]] Fang Wan,[b] Hongji Sun,[a] Yiqing Yang,[a] Wenjun Li,[a] Zheyan Qian,[a] Xuemei Sun,*[a] Peining Chen,*[a] Shiyi Chen,[b] Huisheng Peng*[a]

Figure S1. Photograph showing rolls of continuous CNT sheets. Scale bar, 2 cm.

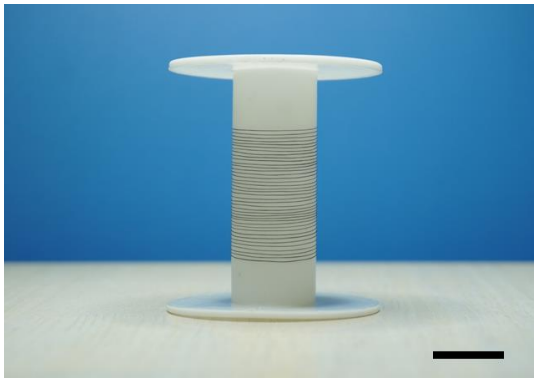

Figure S2. Photograph showing a roll of CNT/PET wrapping fibers. Scale bar, 2 cm.

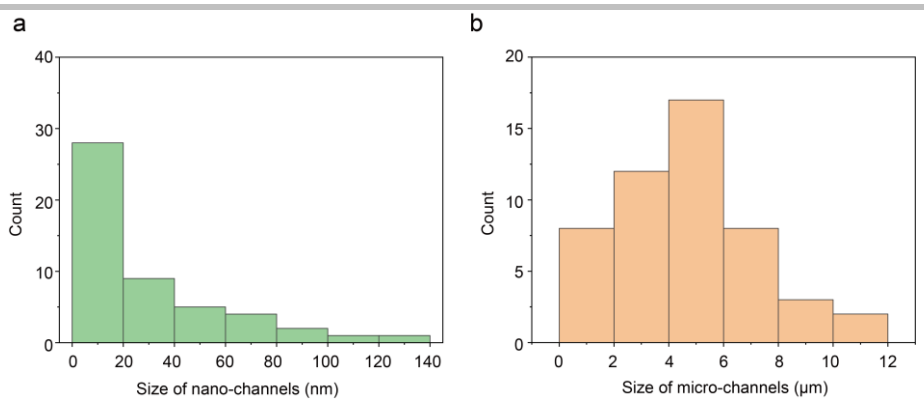

Figure S3. The size distribution of nano-channels (**a**) and micro-channels (**b**) of HCF grafts (n = 50).

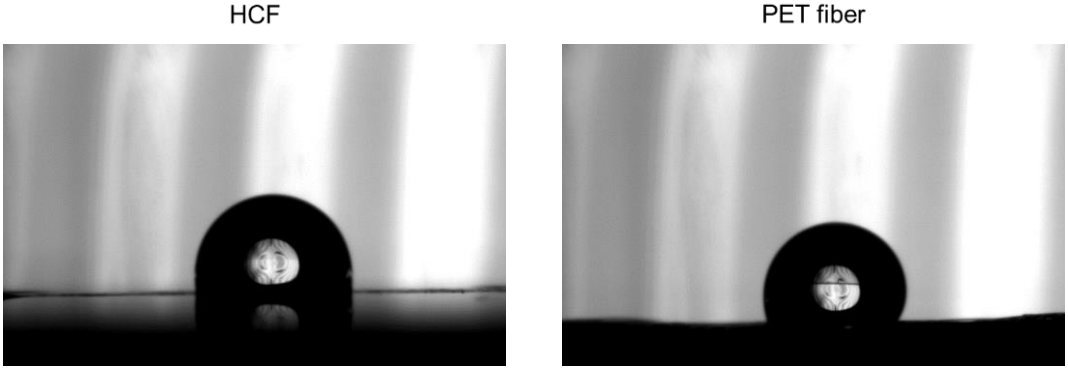

Figure S4. The water contact angles of HCF (Left) and PET fiber (Right).

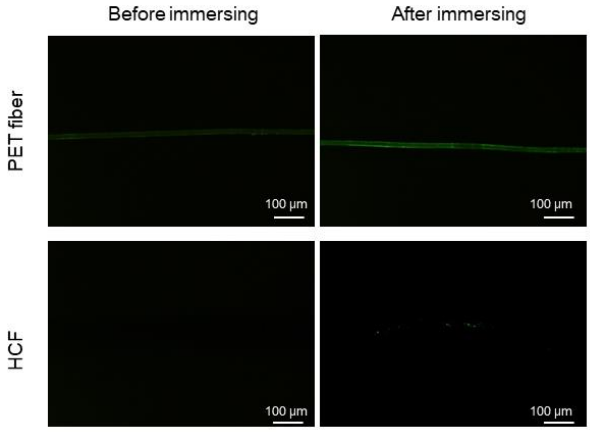

Figure S5. The fluorescence images to show the protein absorption of HCF and PET fibers, after immersing in fluorescein isothiocyanate-bovine serum albumin solution (1 mg/mL, green) for 2 h.

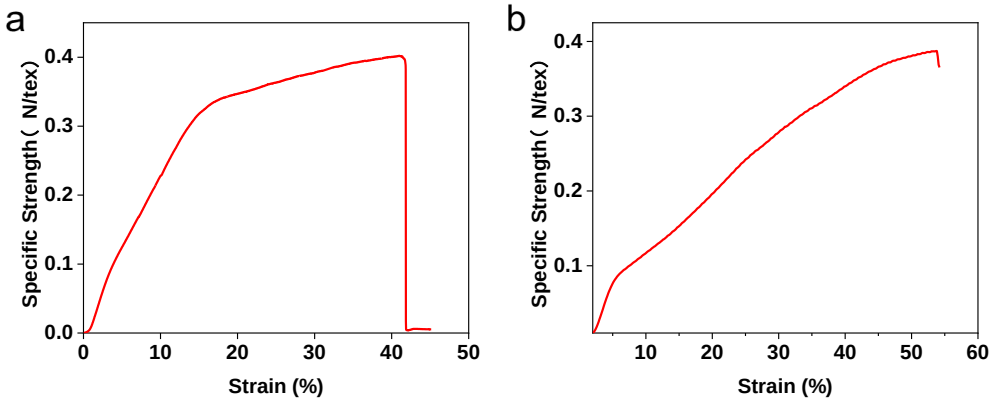

Figure S6. Typical specific strength-strain curves of a single CNT/PET wrapping fiber (**a**) and an HCF (**b**).

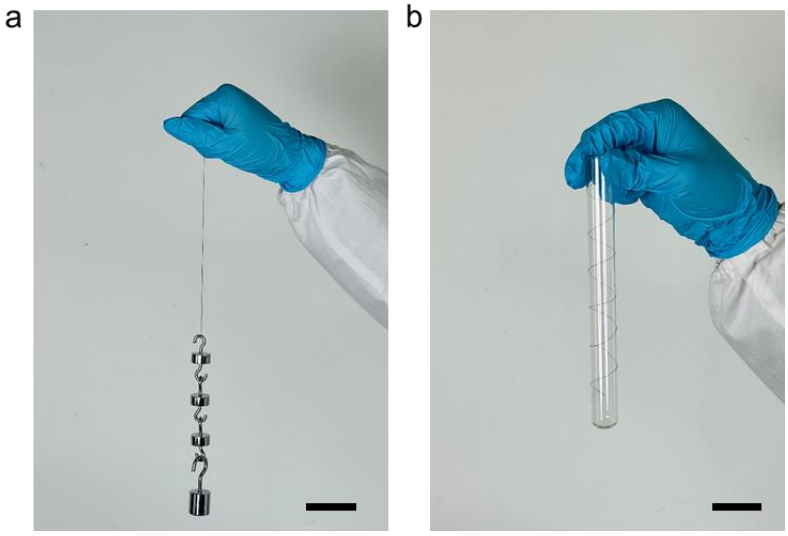

Figure S7. Photographs showing high strength (**a**) and flexibility (**b**) of CNT/PET wrapping fibers. Scale bars, 5 cm (**a**), 3 cm (**b**).

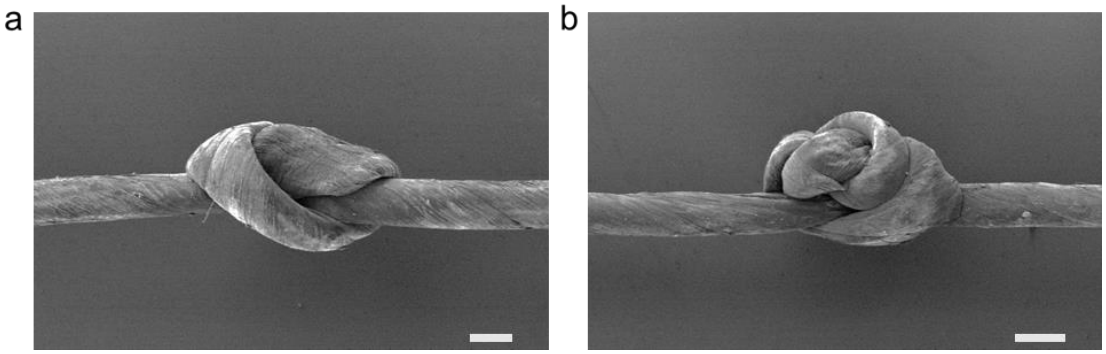

Figure S8. a and **b**, SEM images of a knotted CNT/PET wrapping fiber with once and twice knotted, respectively. Scale bars, 100 μm (**a**), 150 μm (**b**).

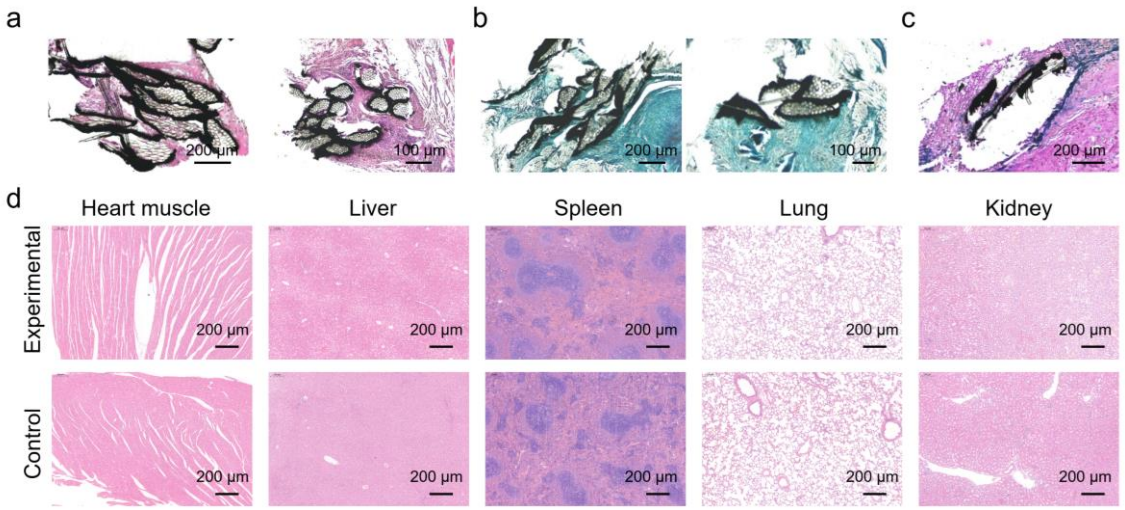

Figure S9. (**a-c**) H&E-stained (a), Golden Masson-stained (b) and Methylene blue-acid magenta-stained (c) images of skeletal muscles with implanted HCFs in rats for 2 weeks. (**d**) H&E-stained images of the internal organs of rats with and without implanted HCFs for 2 weeks.

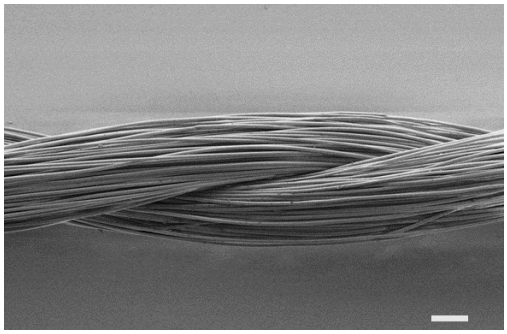

Figure S10. SEM image of bare helical PET fibers. Scale bar, 150 μm.

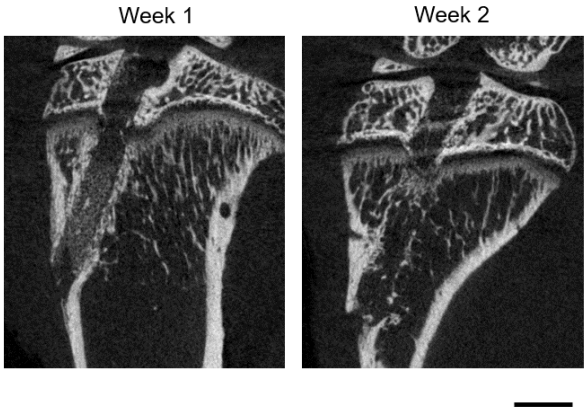

Figure S11. The μCT images of the tibia of rats without any implantable materials after surgery for 1 and 2 weeks. Scale bar, 2 mm.

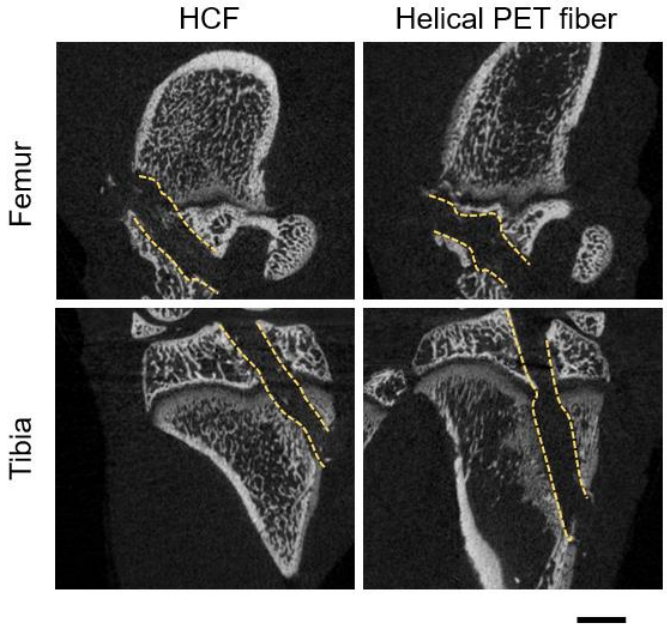

Figure S12. The μCT images of the femur and tibia of rats after surgery for 1 week with HCF and bare helical PET fiber as the ACL grafts. Scale bar, 2 mm.

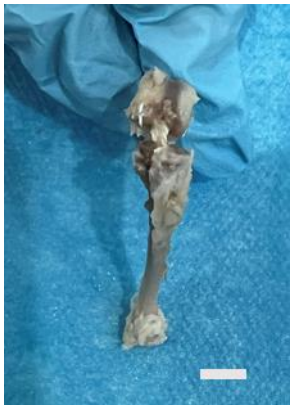

Figure S13. Photograph of the femur-graft-tibia complex containing bare helical PET fiber after surgery for 2 weeks. Scale bar, 5 mm.

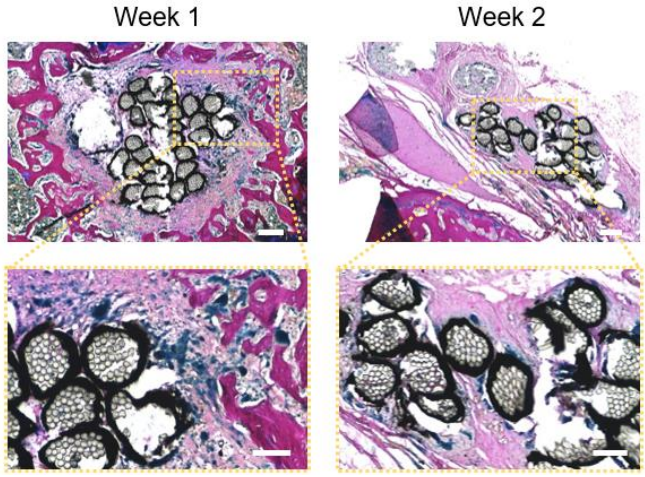

Figure S14. Methylene blue-acid magenta-stained images of bone tunnel implanted with HCF at Week 1 and 2, showing osteoblasts gradually increased at the HCF/host bone interface. Dark blue: osteoblasts; purple grey: osteoid tissue; red: newly formed bone. Scale bars, 200 μm (top), 100 μm (bottom).

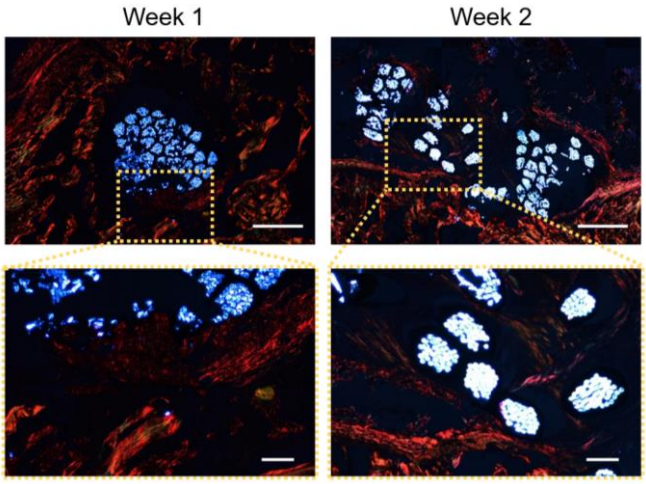

Figure S15. Picrosirius-red-stained images of bone tunnel implanted with HCF at Week 1 and 2 under polarized light, showing anisotropically arranged collagen bundles gradually formed at the interfacial region between HCF and host bone. Scale bars, 500 μm (top), 100 μm (bottom).

Table S1 | Mechanical performance of HCF grafts with previously reported ligaments.

Type	PET fibers	Autografts	PCL fibers	RSF/LAP fibers	HCFs
Stiffness ($N \cdot mm^{-1}$)	65.47±3.81	17-106.5	1.21±0.30	~20	**88.23±9.94**

Strength (MPa)	316.97±2.25	10~53.4	2.0±0.8	~65.8	**323.91±16.70**
Breaking elongation (%)	49.6-64.9	10.6~86.1	11.1±0.8	~35.8	**43.8-67.0**

Note: PCL fibers and RSF/LAP fibers represent polycaprolactone and regenerated silk fibroin/Laponite hybrid fibers, respectively. The performances of PET fibers and HCF at Table S1 were tested and those for other grafts are cited from *ref. S1-3*.

Table S2. Comparison of pull-out forces of our work with previously reported ligaments.

Type	Implantation time	Pull-out force (N)	Ref.
Autografts	3	8.58 ± 2.67	[S4]
Achilles tendon	2	2.2	[S5]
Tendon grafts	2	~8	[S6]
Autografts	3	~10	[S7]
Autografts	2	7.5	[S8]
Stem Cell–Conditioned Medium	4	5.68 ± 1.13	[S9]
Autografts	4	~5	[S10]
Polycaprolactone graft	16	~20	[S11]
Polycaprolactone with growth factors	16	23.1	[S12]
HCF graft	**2**	**20.85 ± 3.91**	**This work**

Reference

[S1] D. A. Brennan, A. Conte, G. Kanski, S. Turkula, X. Hu, M. T. Kleiner, V. Beachley. *Adv. Healthcare Mater.* **2018**, 7, 1701277.

[S2] A. O. Adeoye, F. Mukasheva, S. Smatov, B. Khumyrzakh, S. Kadyr, Z. Shulgau, C. Erisken. *Bioeng. Biotechnol.* **2022**, 10, 969282.

[S3] Dong, Q., Cai, J., Wang, H., Chen, S., Chen, X. *Acta Biomaterialia*, **2020**, 106, 102-113.

[S4] Zong, J. C., Ma, R., Wang, H., Cong, G. T., Lebaschi, A., Deng, X. H., Rodeo. A. S. *Am. J. Sport Med.* **2017**, 45, 1349-1358.

[S5] Geir, A. H., Jan E. M., Lars. N., Finn P. R., Harald S., Sigbjorn D. *J. Orthop. Res.* **2015**, 33, 216-223.

[S6] Fu, S. C., Cheng, W. H., Cheuk, Y. C., Mok, T. Y., Rolf, G. C., Yung, S. H., Chan, K. M. *Knee Surg. Sports Tr. A.* **2013**, 21,1226-1233.

[S7] Ma, R., Schr, M., Chen, T., Sisto, M., Nguyen, J., Voigt, C., Deng, X. H., Rodeo. A. S. *Am. J. Sport Med.* **2018**, 46, 915-923.

[S8] Komiyama, H., Arai, Y., Kajikawa, Y., Yoshida, A., Morihara, T., Terauchi, R., Kida, Y., Fujiwara, H., Kubo, T., Kawata, M., *J. Orthop. Sci.* **2013**, 18, 994-1004.

[S9] Sun, Y., Chen, W., Hao, Y., *Am. J. Sport. Med.* **2019**, 47, 2327-2337.

[S10] Wang, H., Wang, T., Sui, Y., Wang, J., Chen, W., Zhang, Y., *Am. J. Sport. Med.* **2020**, 48, 3515-3524.

[S11] Leong, NL., Kabir, N., Arshi, A., Nazemi, A., Wu, B., McAllister, DR., Petrigliano, FA. Jove-J. *Vis. Exp.* **2015**, 26, 52797.

[S12] Leong, NL., Kabir, N., Arshi, A., Nazemi, A., Wu, B., Petrigliano, FA., McAllister, DR. *Tissue Eng Part A.* **2015**, 21, 1859-1868.

Caption for Supplementary Movie

Supplementary Movie | Movement of a rat with HCF graft as reconstructed ACL.